Supporting Information for

Uniform Growth of Sub-5 nm High-κ Dielectrics on MoS_2 Using Plasma-enhanced Atomic Layer Deposition

*Katherine M. Price[1], Kirstin E. Schauble[2], Felicia A. McGuire[1], Damon B. Farmer[3], and Aaron D. Franklin[1,4]**

[1]Department of Electrical and Computer Engineering, Duke University, Durham, NC 27708, USA
[2]Department of Electrical and Computer Engineering, Seattle University, Seattle, WA 98122, USA
[3]IBM T. J. Watson Research Center, Yorktown Heights, NY 10598, USA
[4]Department of Chemistry, Duke University, Durham, NC 27708, USA

* Corresponding author. Email: aaron.franklin@duke.edu

CONTENTS

8. Impact of thermal exposure during PEALD Al_2O_3
9. Effect of thermal ALD Al_2O_3 on back-gated characteristics
10. Impact of thermal exposure during PEALD HfO_2
11. Effect of thermal ALD HfO_2 on back-gated characteristics
12. XPS C 1s peak used for calibration for PEALD/ALD HfO_2 and Al_2O_3
13. Top-gate fabrication process flow
14. EDS of cross-section STEM
15. CV curves

1. Experimental setup

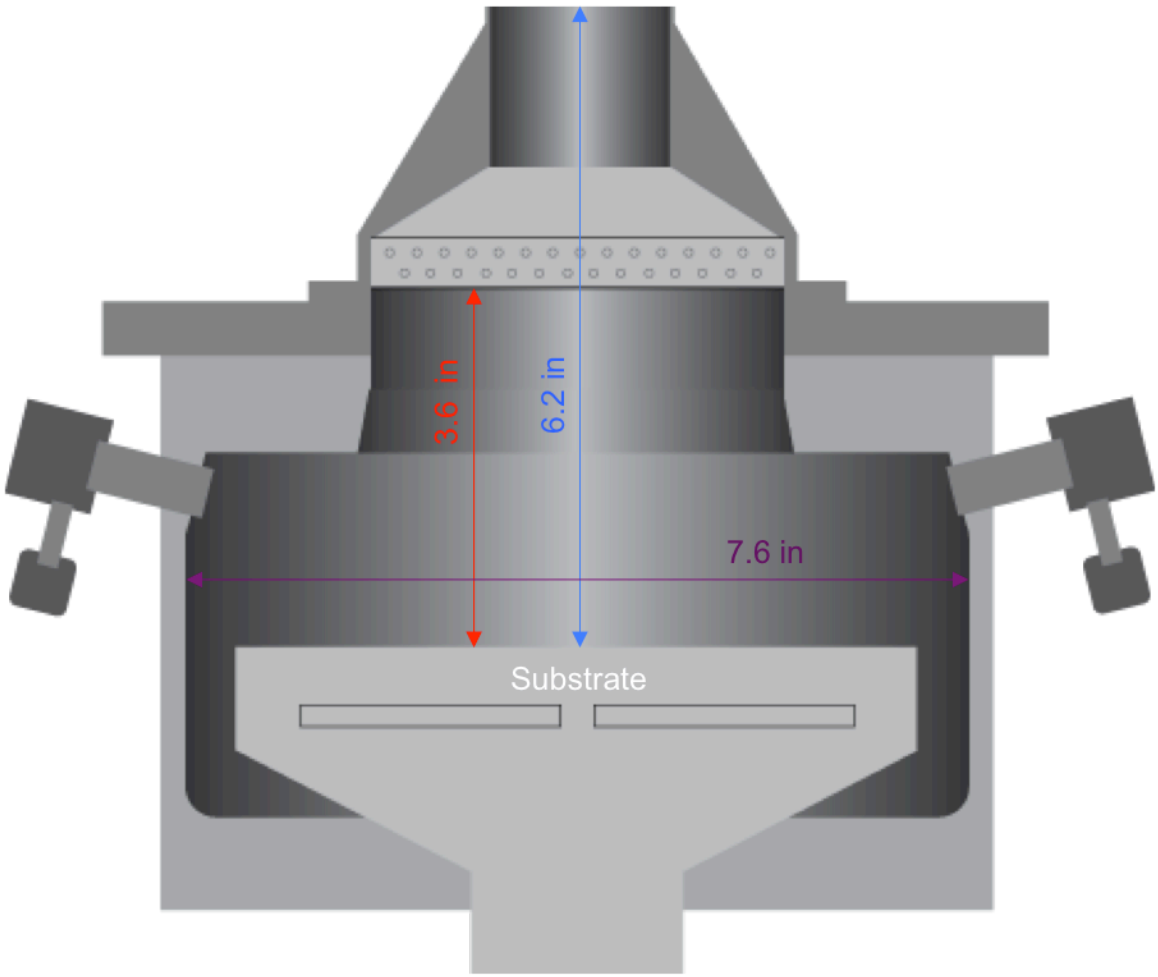

Fig S1. Schematic of the PEALD and ALD chamber, to scale. The chamber is 7.6 inches in diameter (purple). The remote plasma used in the PEALD process is formed 6.2 inches away from the substrate (blue) and travels through the showerhead located 3.6 inches above the substrate (red). The showerhead openings are only around the perimeter to keep highly energetic radicals from the plasma from having line-of-sight access to the substrate.

The atomic layer deposition (ALD) and plasma-enhanced ALD (PEALD) were performed in the same custom-designed Kurt J. Lesker reaction chamber (Fig. S1). The ALD precursors used for Al_2O_3 [HfO_2] were trimethylaluminum (TMA) [tetrakis (ethylmethylamino)hafnium (TMDAH) heated to 85˚C] and water vapor. The PEALD

used the same precursors as ALD, except the oxidant was an oxygen plasma. The oxygen plasma is a remote RF plasma (sustained at 400 W with Ar) formed by first striking an Ar plasma for 10 msec followed by flowing O_2 into the plasma at a rate of 9 sccm for 6000 msec in tandem with the constant stream of Ar. Once the O_2 pulse is complete, the Ar plasma remains on for another 1000 msec before turning off, and the chamber is then purged for 5000 msec. The plasma is formed 6.2 inches above the sample and travels through a showerhead, located 3.6 inches above the sample, which filters out the most energetic plasma species and prevents highly energetic radicals from the plasma from having line-of-sight access to the substrate. All samples are loaded into the chamber and given 1200 sec to reach thermal equilibrium before the ALD/PEALD process begins. The ALD/PEALD follows the typical series of steps: pulse precursor, purge precursor, pulse oxidant, purge oxidant. ALD Al_2O_3 films grown at 220˚C and 332˚C had the following pulse/purge times: 40 msec pulse TMA, 10,000 msec purge, 140 msec pulse H_2O, 10,000 msec purge. PEALD Al_2O_3 films at 220˚C and 332˚C had a 40 msec pulse TMA, 10,000 msec purge, 6000 msec O_2 plasma, 5000 msec purge. ALD HfO_2 films grown at 220˚C and 332˚C had the following pulse/purge times: 200 msec pulse TMDAH , 20,000 msec purge, 140 msec pulse H_2O, 10,000 msec purge. PEALD HfO_2 films at 220˚C and 332˚C had a 200 msec pulse TMDAH, 10,000 msec purge, 6000 msec O_2 plasma, 5000 msec purge. At 120˚C all above purge times were doubled (excluding the O_2 plasma purge time) in order to allow the less energetic precursors sufficient time to be purged to ensure no CVD reactions occurred.

AFM was done using a digital instruments dimension 3100 using Bruker TESPA – HAR AFM tips. XPS was performed using a Kratos analytical axis ultra with Al K

alpha radiation with a pass energy of 15 eV. Ellipsometry measurements were done *ex situ* using an Eoolam M88 ellipsometer. The cross-section STEM images were taken using a FEI Titan 80-300 probe aberration corrected STEM.

2. Growth per cycle of PEALD/ALD Al_2O_3 and HfO_2

Table S1. Growth per cycle of PEALD and ALD for Al_2O_3 and HfO_2 on SiO_2 obtained using *ex situ* ellipsometry.

Film	Temperature [˚C]	GPC [nm/cycle]
ALD HfO_2	**120**	**0.123**
PEALD HfO_2	**120**	**0.124**
ALD Al_2O_3	**220**	**0.090**
PEALD Al_2O_3	**220**	**0.111**

3. AFM of MoS_2 before/after PEALD HfO_2

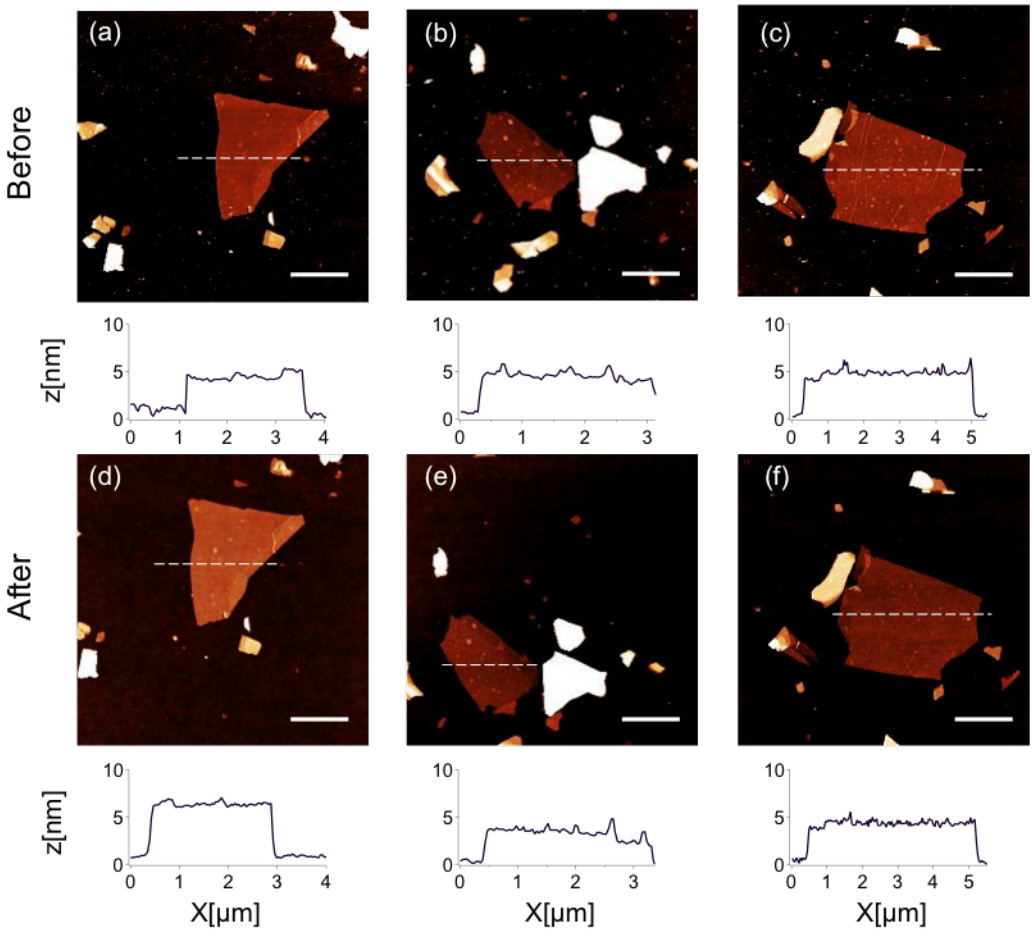

Figure S3. Comparison of MoS_2 flake thickness before and after 28 cycles of PEALD HfO_2 on MoS_2 at 120˚C. AFM images with line-scan height profiles for (a-c) as-exfoliated MoS_2 flakes and (d-f) MoS_2 flakes after 28 cycles PEALD HfO_2. Scale bars are 2 μm.

4. 1 μm^2 scan areas on MoS_2 after PEALD/ALD Al_2O_3 (including RMS)

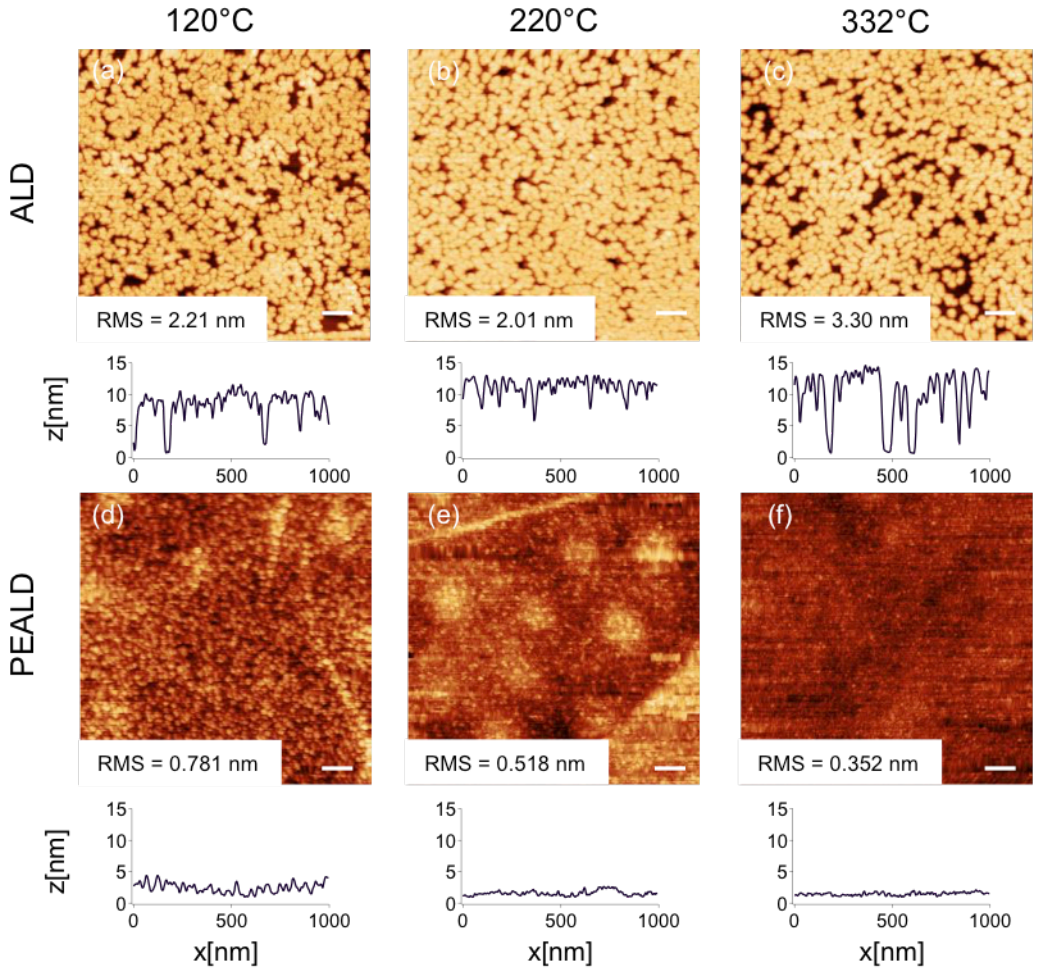

Figure S4. Comparison of ALD and PEALD Al_2O_3 on MoS_2 at different temperatures. AFM images, line-scan height profiles, and RMS values after 125 cycles (~10 nm) of ALD and PEALD Al_2O_3 on MoS_2. ALD Al_2O_3 at (a) 120°C, (b) 220°C, and (c) 332°C on MoS_2. PEALD Al_2O_3 at (d) 120°C, (e) 220°C, and (f) 332°C on MoS_2. All MoS_2 flakes are nominally 6-8 nm thick. Scale bars are 100nm.

5. AFM of PEALD HfO_2

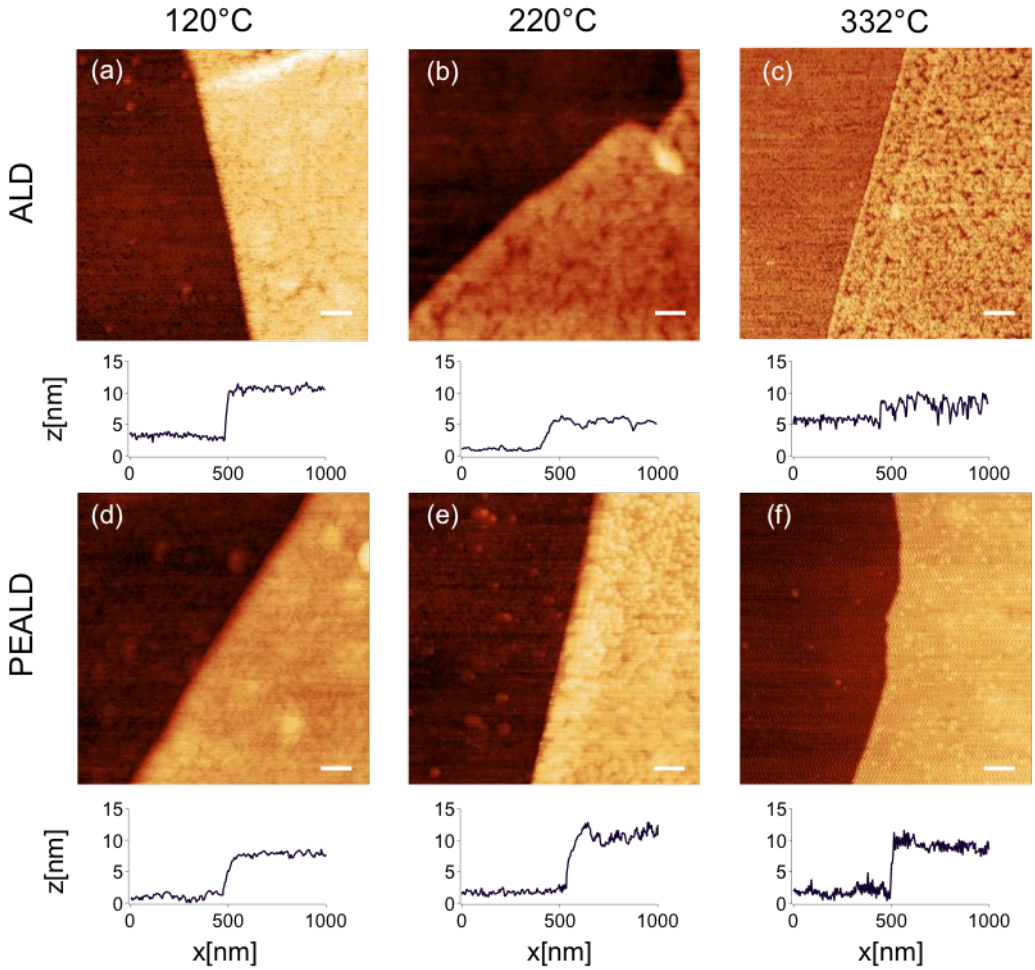

Figure S5. Comparison of ALD and PEALD HfO_2 on MoS_2 at different temperatures. Atomic force microscopy (AFM) images and line-scan height profiles after 115 cycles (~10 nm) of ALD and PEALD HfO_2 on MoS_2. ALD HfO_2 at (a)120°C, (b) 220°C, and (c) 332°C on MoS_2. PEALD HfO_2 at (d) 120°C, (e) 220°C, and (f) 332°C on MoS_2. Scale bars are 100nm.

6. 1 μm^2 scan areas on MoS_2 after PEALD/ALD HfO_2 (including RMS)

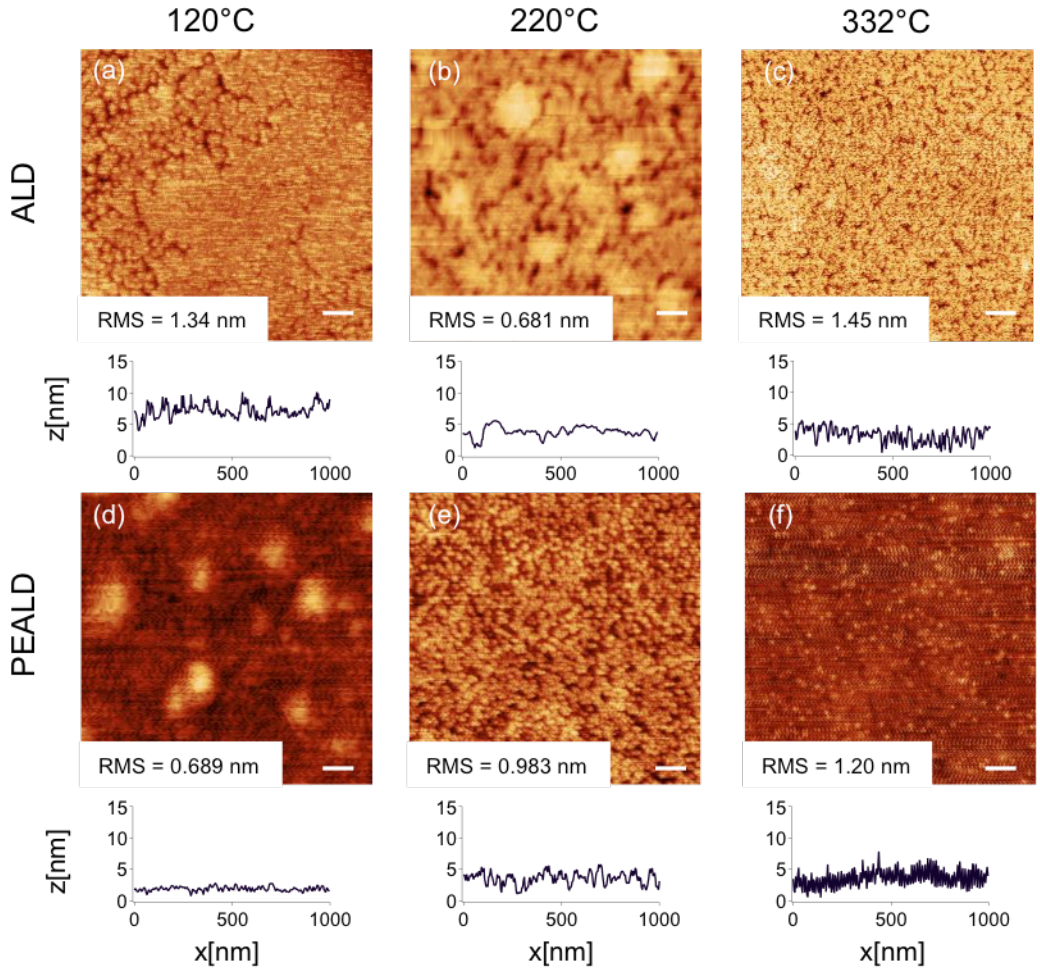

Figure S6. Comparison of ALD and PEALD HfO_2 on MoS_2 at different temperatures. AFM images, line-scan height profiles, and RMS values after 115 cycles (~10 nm) of ALD and PEALD HfO_2 on MoS_2. ALD HfO_2 at (a) 120°C, (b) 220°C, and (c) 332°C on MoS_2. PEALD HfO_2 at (d) 120°C, (e) 220°C, and (f) 332°C on MoS_2. All MoS_2 flakes are nominally 6-8 nm thick. Scale bars are 100nm.

7. 1 μm^2 scan areas on MoS_2 of scaled down PEALD/ALD HfO_2 and Al_2O_3 (including RMS)

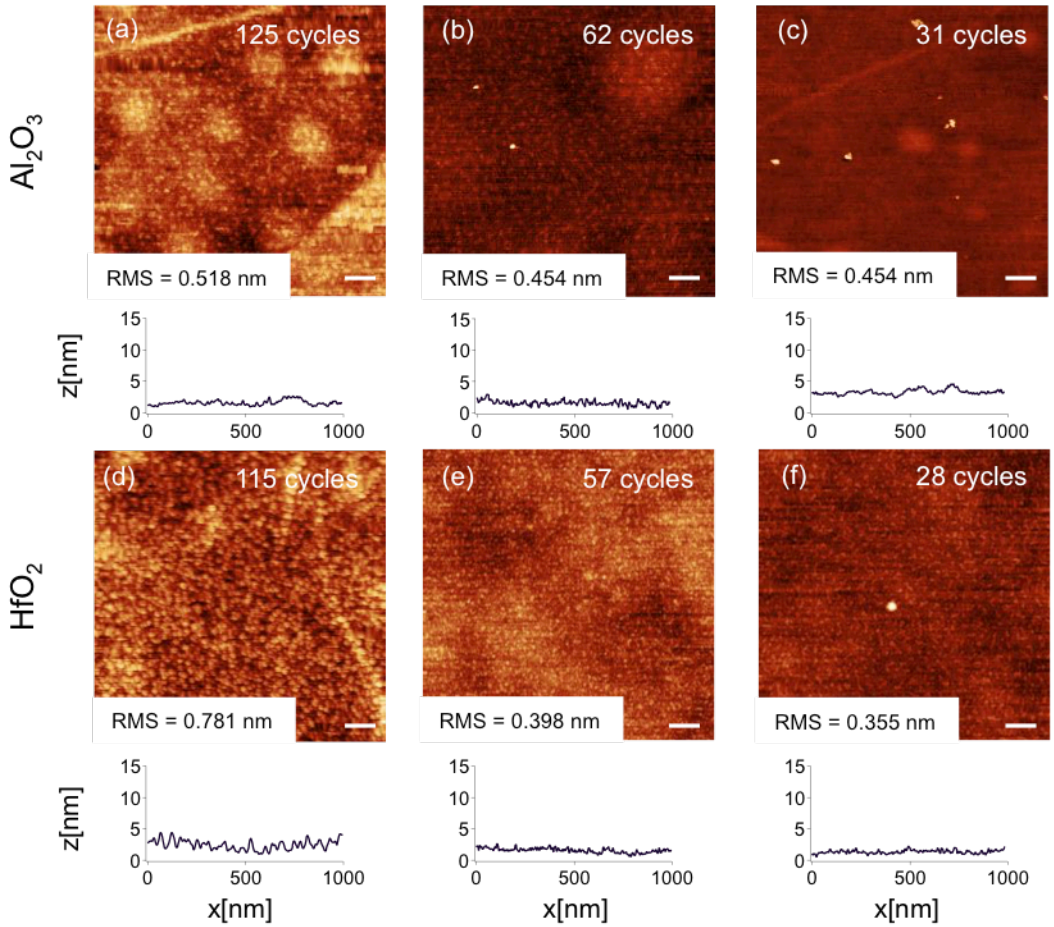

Figure S7. Scaling down of PEALD Al_2O_3 and HfO_2 on MoS_2. AFM images, line-scan height profiles, and RMS values of: PEALD Al_2O_3 for (a) 125 cycles (b) 62 cycles, and (c) 31 cycles (~3.4 nm); PEALD HfO_2 for (d) 115 cycles (e) 57 cycles, and (f) 28 cycles (~3.5 nm). Scale bars are 100 nm.

8. Impact of thermal exposure during PEALD Al_2O_3

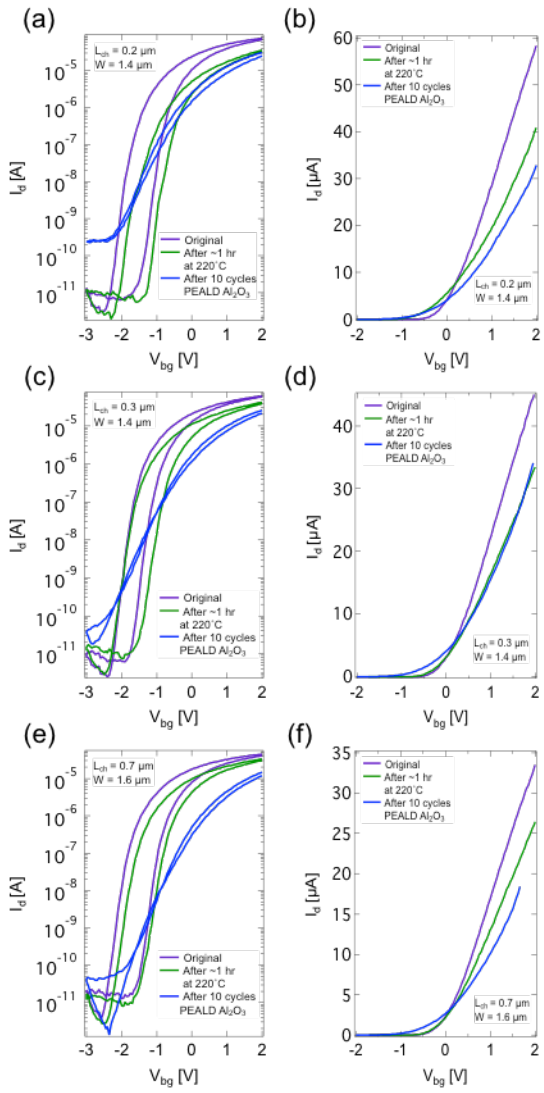

Figure S8. Impact of temperature effects during PEALD (~1 hr at 220˚C) on Ni-MoS_2 contact interface and impact of PEALD Al_2O_3 (10 cycles) on MoS_2 FET performance. Back-gated MoS_2 FETs were first fabricated and characterized. Three different devices with L_{ch} = 200 nm (a-b), 300 nm (c-d), and 700 nm (e-f) were tested with subthreshold (a, c, e) and transfer (b, d, f) curves given. Generally, the thermal exposure of the PEALD process (first done without any actual PEALD), lead to a slight increase in *SS* and little change in hysteresis for the off-state, with a notable decrease in performance (g_m and I_{on}) for the on-state. After exploring this annealing effect, 10 cycles of PEALD Al_2O_3 were deposited and the devices were characterized again, showing further increase in SS, decrease in I_{ON}/I_{OFF}, and reduction in hysteresis for the off-state. Meanwhile, the PEALD Al_2O_3 generally resulted in further decrease in g_m and I_{ON}. Note that V_{ds} = 1V for all curves and the curves in (b), (d) and (f) are all shifted so that the threshold voltage (V_T) is 0V in order to compare the on-state performance.

9. Effect of thermal ALD Al_2O_3 on back-gated characteristics

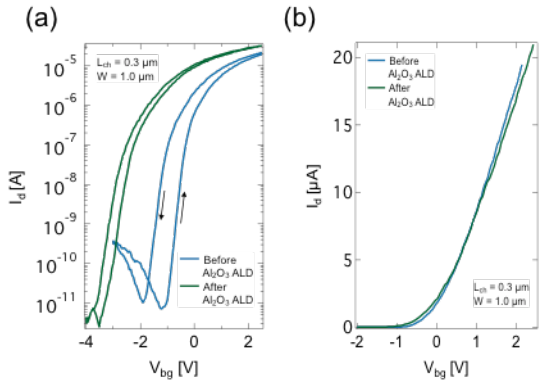

Figure S9. Impact of thermal ALD Al_2O_3 on MoS_2 back-gated FET electrical properties (V_{ds} = 1V). (a) Subthreshold hysteresis curves from the same device before and after thermal ALD Al_2O_3 (250 cycles) showing an increase in *SS*, but decrease in hysteresis. (b) Transfer curves (same device as in (a)) before and after thermal ALD Al_2O_3 show almost no change in transconductance and I_{ON}.. Note that the curves in (b) are all shifted so that the threshold voltage (V_T) is 0 V for all curves in order to compare the on-state performance.

10. Impact of thermal exposure during PEALD HfO_2

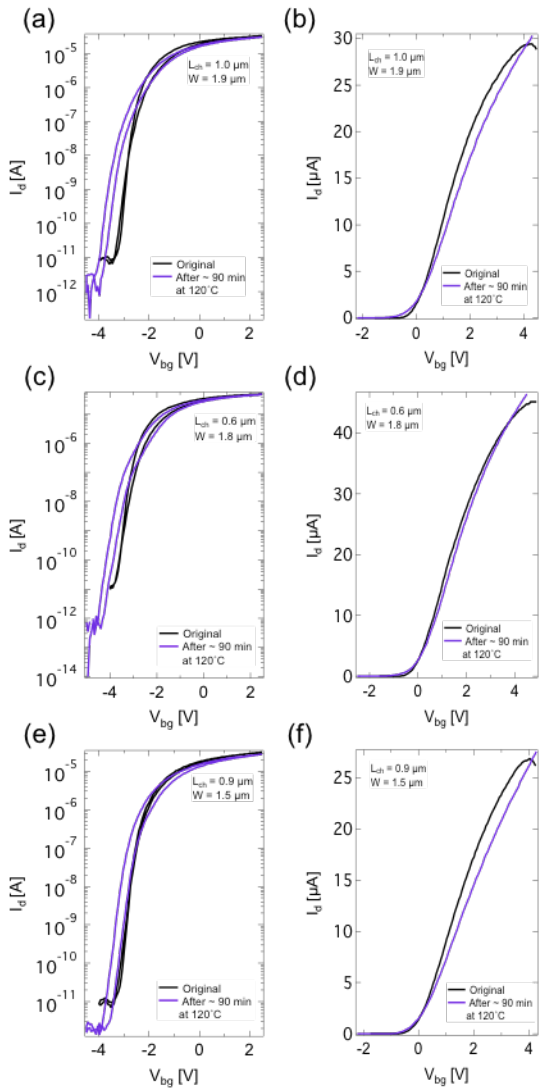

Figure S10. Impact of temperature effects during PEALD (~90 min at 120˚C) on Ni-MoS_2 contact interface by monitoring changes in MoS_2 FET performance. Back-gated MoS_2 FETs were first fabricated and characterized. Three different devices were tested with subthreshold (a, c, e) and transfer (b, d, f) curves given. Generally, the thermal exposure of the PEALD process (done without any actual PEALD), led to a slight increase in SS with a slight decrease in performance (g_m and I_{on}) for the on-state. Note that V_{ds} = 1V for all curves and the curves in (b), (d) and (f) are all shifted so that the threshold voltage (V_T) is 0V in order to compare the on-state performance.

11. Effect of thermal ALD HfO_2 on back-gated characteristics

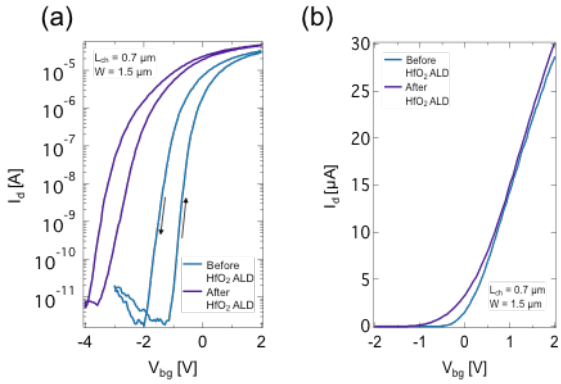

Figure S11. Impact of thermal ALD HfO_2 on MoS_2 back-gated FET electrical properties. (V_{ds} = 1V) (a) Subthreshold hysteresis curves from the same device before and after thermal ALD HfO_2 (230 cycles) showing a slight increase in *SS* and decrease in hysteresis. (b) Transfer curves (same device as in (a)) before and after thermal ALD HfO_2 show almost no change transconductance and I_{ON}.. Note that the curves in (b) are all shifted so that the threshold voltage (V_T) is 0V for all curves in order to compare the on-state performance.

12. XPS C 1s peak used for calibration for PEALD/ALD HfO_2 and Al_2O_3

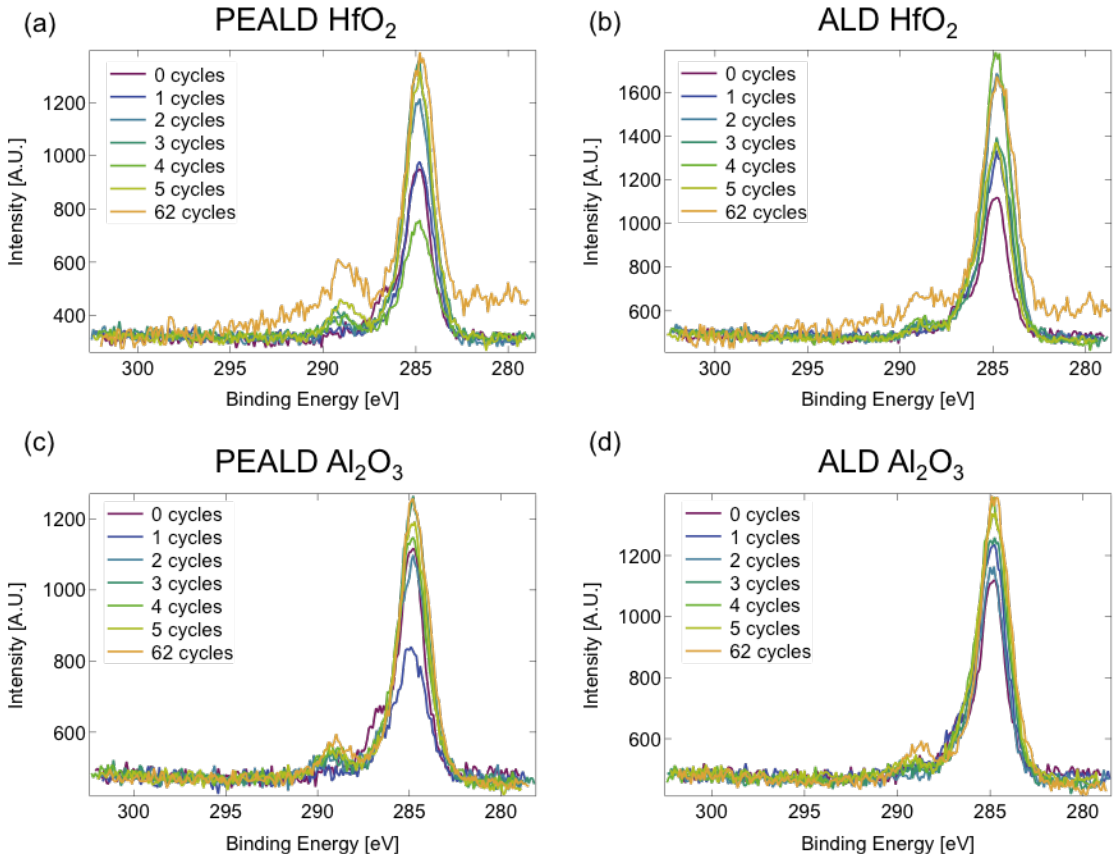

Figure S12. XPS spectra of C 1s peak for (a) PEALD HfO_2 (120˚C), (b) ALD HfO_2 (120˚C),, (c) PEALD Al_2O_3 (220˚C),, and (d) ALD Al_2O_3 (220˚C).

13. Top-gate fabrication process flow

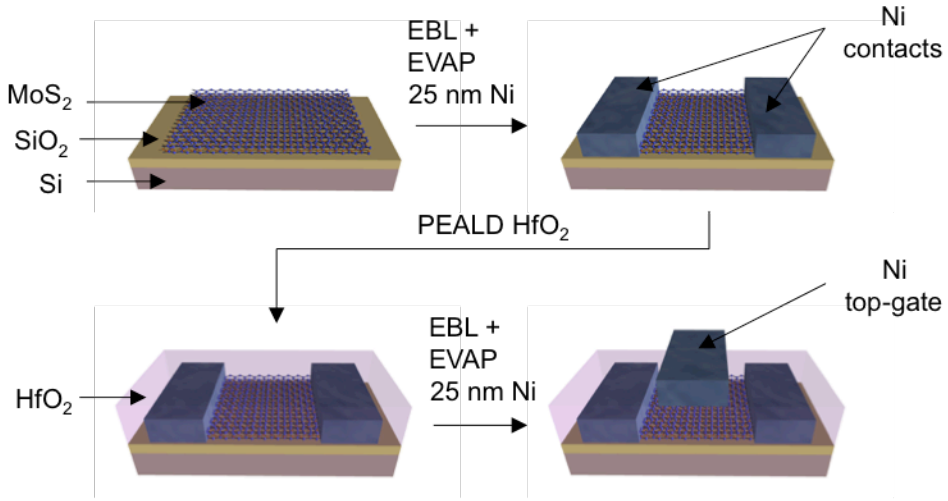

Figure S13. MoS_2 was exfoliated onto 90 nm SiO_2/Si wafers and flakes of thickness ranging from 5-8 nm were selected. Electron-beam lithography (EBL) was used to define the contacts and pads. Electron-beam evaporation was carried out to deposit 25 nm Ni for the contacts and 2 nm Ti/ 20 nm Pd/ 20 nm Au for the pads. PEALD was used to deposit HfO_2 as the gate dielectric with a thickness of ~3.4 nm. EBL was then used to define an underlapped top-gate. Electron-beam evaporation was carried out to deposit 25 nm Ni for the top-gate.

14. EDS of cross-section STEM

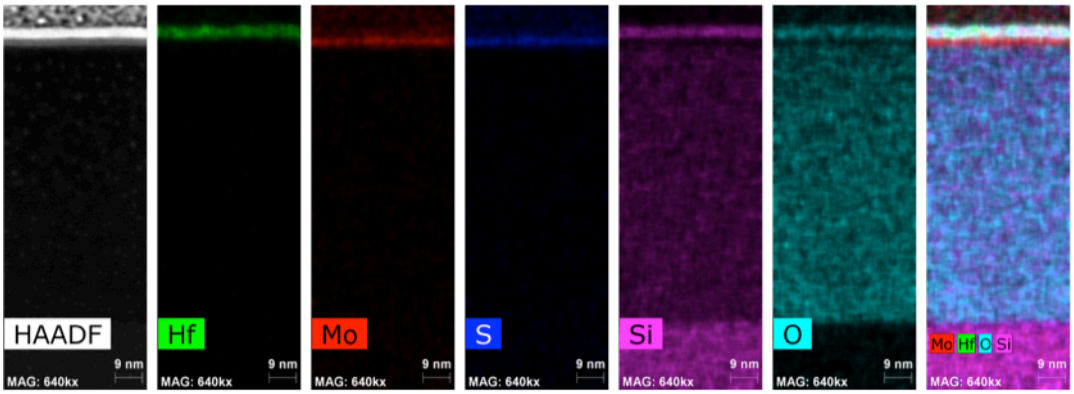

Figure S14. EDS of cross-sectional STEM image. Hf, Mo, S, Si, and O images are shown independently and collectively, indicating the areas that contain each of the respective elements.

15. CV curves

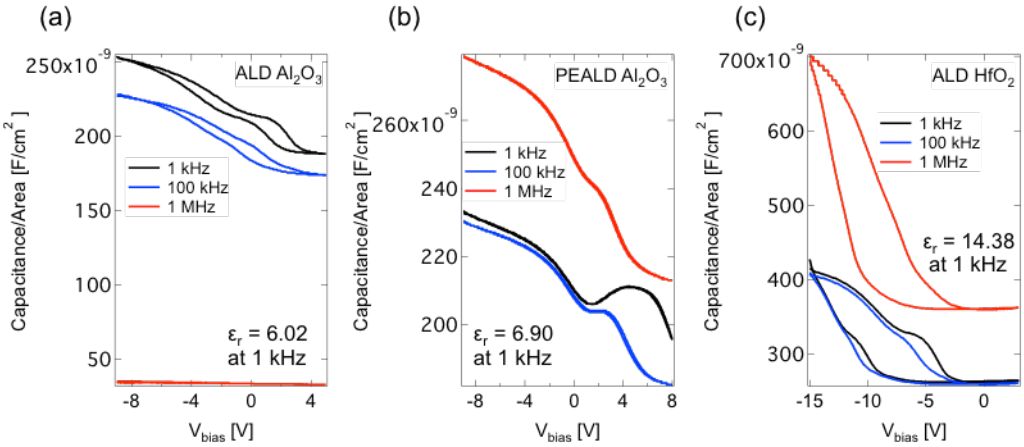

Figure S15. C-V curves of ALD/PEALD Al_2O_3 and ALD HfO_2 with extracted relative permittivity at 1 kHz. (a) Frequency-dependent C-V curve from Si/ALD Al_2O_3 (220˚C)/Al capacitor with a relative permittivity of 6.02 at 1 kHz. (b) Si/PEALD Al_2O_3 (220˚C)/Al capacitor with a relative permittivity of 6.90 at 1 kHz. (c) Si/ALD HfO_2 (120˚C)/Al capacitor with a relative permittivity of 14.38 at 1 kHz.